PHILOSOPHICAL TRANSACTIONS OF THE ROYAL SOCIETY A

Phil. Trans. R. Soc. A (2008) **366**, 2871–2880
doi:10.1098/rsta.2008.0080
Published online 6 June 2008

Do superconductors change as fast as possible when quenched?

By Ray Rivers[1,*], Roberto Monaco[2,3], Jesper Mygind[4], Morten Aaroe[4] and Valery Koshelets[5]

[1]*Blackett Laboratory, Imperial College London, London SW7 2AZ, UK*
[2]*Istituto di Cibernetica del C.N.R., 80078 Pozzuoli, Italy*
[3]*Unitá INFM-Dipartimento di Fisica, Universitá di Salerno, 84081 Baronissi, Italy*
[4]*Department of Physics, B309, Technical University of Denmark, 2800 Lyngby, Denmark*
[5]*Institute of Radio Engineering and Electronics, Russian Academy of Science, Mokhovaya 11, Building 7, 125009 Moscow, Russia*

If superconductors change as fast as possible as they pass through a phase transition, then the initial domain structure is constrained by causality. We shall see that Josephson junctions do indeed display such behaviour. However, we shall argue that causal bounds arise through the Gaussian nature of the order parameter, which can be thought of as a consequence of instabilities growing as fast as possible.

Keywords: Josephson tunnel junctions; fluxons; Kibble–Zurek scenario

1. Introduction: causality and scaling behaviour

The Kibble–Zurek (KZ) scenario for continuous phase transitions proposes that transitions take effect as fast as possible, i.e. the domain structure initially matches causal horizons. Since causality is ubiquitous, this proposition, if true, would apply equally to both the early Universe and laboratory-based condensed matter systems.

Causality necessarily leads to a 'domain' structure owing to the inability of a field to order itself instantaneously (Kibble 1976). To take this further, Kibble (1980) and Zurek (1985, 1996) made two assumptions for continuous transitions, for which the adiabatic correlation length $\xi_{\rm ad}(T)$ diverges at the critical temperature $T_{\rm c}$. In reality, correlation lengths cannot become infinite because there is a maximum speed at which the field can order itself. The first assumption is that the maximum value that the physical correlation length ξ can take is $\bar{\xi}=\xi_{\rm ad}(T(\bar{t}))$ for some appropriate time $\bar{t}$, most simply that at which the rate of change of $\xi_{\rm ad}(T(t))$ is as fast as causality permits.

* Author for correspondence (r.rivers@imperial.ac.uk).

One contribution of 16 to a Discussion Meeting Issue 'Cosmology meets condensed matter'.

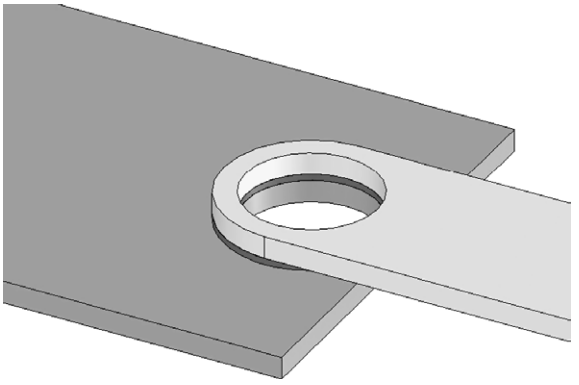

Figure 1. An idealized AJTJ. The flux passing through the oxide layer that surrounds a superconducting electrode will be trapped below T_c.

Whether $\bar{\xi}$ is observable directly, or not, depends on the nature of the frustration of the order parameter as it moves from one ground state to the next. In cases of interest, the order parameters cannot 'untwist' at these domain boundaries owing to conserved topological charges. The second KZ assumption is that if the symmetry breaking in the transition permits such defects, then $\bar{\xi}$ is their separation at the time of their production, which can be checked experimentally.

With $T(t{=}0) = T_c$, the quench time (inverse quench rate) τ_Q is defined by $\tau_Q = -T_c/\dot{T}(0)$, where the dot denotes differentiation with respect to time. The KZ assumptions

$$|\dot{\xi}(T(\bar{t}))| \approx c(T(\bar{t})), \qquad \bar{\xi} \approx \xi(T(\bar{t})) \tag{1.1}$$

lead to a scaling behaviour with τ_Q for $\bar{\xi}$ of the form

$$\bar{\xi} \approx \xi_0(\tau_Q/\tau_0)^{\sigma}. \tag{1.2}$$

The scaling exponent σ in (1.2) depends *only* on the equilibrium critical indices of the system, whereas the parameters ξ_0 and τ_0 have to be determined from the characteristics of the particular sample being tested. In this way, the universality classes of adiabatic systems become the universality classes of strongly non-equilibrium systems.

Superconductors seem to be the natural candidates to test (1.2) directly, since they have vortices (e.g. Abrikosov vortices) as topological defects. However, the scaling behaviour of (1.2), based on the density of Cooper pairs, is too simple (Zurek 1996). There is a further mechanism (Hindmarsh & Rajantie 2000) for producing spontaneous flux, in which the long-wavelength modes of the magnetic field will fall out of equilibrium at the quench. This additional flux does not satisfy (1.2). It is to avoid this problem that we have chosen to work with annular Josephson tunnel junctions (AJTJs), for which the topological charge is the magnetic flux carried by a vortex 'fluxon' in the plane of the oxide layer between the two superconductors that make up the Josephson tunnel junction (JTJ). The angle subtended by the oxide is so small that there is no additional flux to concern us.

An idealized AJTJ consisting of two electrodes made from identical superconductors is shown in figure 1. Above T_c, the magnetic flux lines arising from the fluctuations of the electromagnetic field can pass easily through the (now) conducting electrodes. On cooling through T_c, those flux lines that pass through the

oxide layer but circle a superconductor (and are thereby expelled from it) are trapped in the oxide. The total flux is conserved. It can be measured at any time after the quench, and its dependence on quench time τ_Q can be determined.

The effective order parameter field of the bulk superconductors is $\Psi = \rho^{1/2} e^{i\phi}$, where ρ is the density of Cooper pairs. If x is the (periodic) coordinate along the ring, we assume continuity in ρ across the oxide, but allow for a discontinuity $\phi(x) = \phi_+(x) - \phi_-(x)$ in phase. The Cooper pair tunnelling current through the oxide gives a transverse current $J = J_c \sin \phi(x)$, the Josephson current.

To a good approximation, this Anderson plasma mode $\phi(x)$ satisfies the sine-Gordon equation (Barone & Paterno 1982)

$$\frac{1}{\bar{c}^2}\frac{\partial^2 \phi}{\partial t^2} - \frac{\partial^2 \phi}{\partial x^2} + \frac{1}{\lambda_J^2}\sin \phi = 0. \tag{1.3}$$

In (1.3), the speed of propagation of the plasma excitations is the Swihart velocity $\bar{c}$, effectively the speed of light in the oxide layer. The Josephson coherence length of the plasma modes is $\lambda_J \propto J_c^{-1/2}$. On quenching the system through T_c, the field finds itself in one of the many degenerate ground states $\phi = 2\pi n$ (integer n). If we follow the phase around the inner boundary of the junction we shall find 'kinks' in ϕ where it changes value by $\pm 2\pi$ over a length $O(\lambda_J)$. When this happens, the Josephson current changes its direction, showing the presence of a unit of magnetic flux leaving the oxide layer. This is a Josephson fluxon.

With the Swihart velocity to set causal horizons and the Josephson coherence length to characterize the separation of fluxons, we can apply the KZ scenario directly to determine the initial, and hence final, fluxon probability. In practice, it is most convenient to consider quenches of a small junction of perimeter C (the interior circumference of figure 1), with $\bar{\xi} > C$. If f_1 and f_{-1} are the probabilities of seeing a single fluxon or antifluxon, respectively, then we expect scaling behaviour of the form

$$\bar{f}_1 = f_1 + f_{-1} \approx C/\bar{\xi} = (C/\xi_0)(\tau_Q/\tau_0)^{-\sigma} < 1, \tag{1.4}$$

provided $\bar{f}_1$ is sufficiently smaller than unity.

The exponent σ depends on the details of the fabrication of the JTJs. Ours are based on Nb, a *strong-coupling* superconductor. In practice, high-quality barriers are achieved by depositing a thin Al overlay onto the Nb base electrode which will be only partially oxidized, leaving an Nb–Al bilayer underneath having a non-Bardeen–Cooper–Schrieffer temperature dependence of the energy gap and of the density of states. This 'proximity effect' leads to the coherence length diverging near T_c as $\xi(T) = \lambda_J(T) \approx \xi_0(1 - T/T_c)^{-1} \approx \xi_0 \tau_Q / t$ in the vicinity of T_c ($t > 0$; Golubov *et al.* 1995).

For long ideal JTJs, the Swihart velocity vanishes at T_c, whereas for realistic JTJs it just becomes very small. As a result, we assume $\bar{c}(t) = \bar{c}_{nn}$ near the transition temperature where $\bar{c}_{nn}$ is the speed of the light in a microstrip line made of normal metals. We still have approximate critical slowing down insofar as $\bar{c}_{nn}$ is much smaller than the zero-temperature Swihart velocity. Solving the causality equation (1.1) with a non-vanishing Swihart velocity yields $\bar{t} = \sqrt{\tau_0 \tau_Q}$, where $\tau_0 = \xi_0/\bar{c}_{nn}$ ($\tau_0 = O(1\ \text{ns})$), whence

$$\bar{\xi} = \xi_0 (\tau_Q/\tau_0)^{1/2}. \tag{1.5}$$

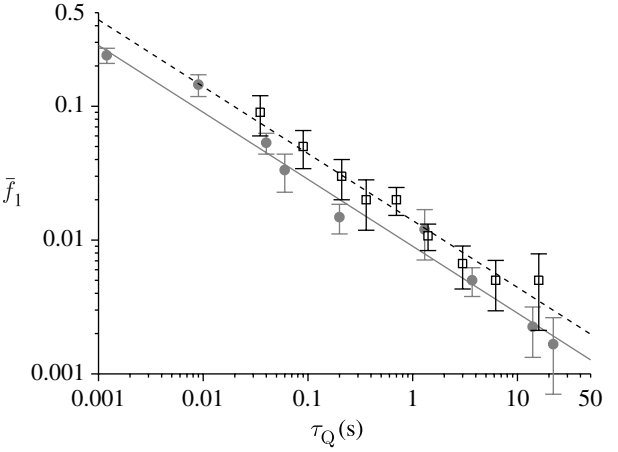

Figure 2. Log–log plot of the frequency of trapping single fluxons $\bar{f}_1$ versus quench time τ_Q for AJTJs of circumferences 0.5 (circles) and 1.5 mm (squares). The best fits through the data (solid and dashed lines) are for $\sigma=0.5$.

That is, the probability $\bar{f}_1$ for spontaneously producing one fluxon (or antifluxon) in the quench is predicted to scale with the quench time τ_Q with scaling exponent $\sigma=0.5$. (This is in contrast to weak-coupling junctions with complete critical slowing down, which give $\sigma=0.25$ (Kavoussanaki *et al.* 2000).)

Several experiments have now been performed by us, which show this scaling behaviour (Monaco *et al.* 2002, 2003, 2006*a*,*b*). In figure 2, we show some results from the most recent, which show scaling with an exponent $\sigma=0.5$ to high accuracy within errors for annuli with circumferences of 0.5 and 1.5 mm.

These data look like a striking confirmation of the effects of causality on the evolution of phase transitions. However, the picture is rather more subtle than the simplest KZ scenario suggests. In particular, it is also necessary to understand fluxon production in the presence of an external magnetic field, i.e. explicit symmetry breaking.

2. Fluxon production in an external magnetic field

In the experiments of figure 2, considerable attention has been paid to the shielding of the junction against stray magnetic fields. Nonetheless, we still cannot preclude the possibility of stray magnetic fields in the experimental equipment.

In fact, in presenting the data in figure 2 we have taken the effects of static stray fields empirically into account, by applying an external magnetic field B perpendicular to the junction plane until such stray fields as may be present are neutralized. This choice of field orientation is sufficient because a transverse field is more effective in modulating the junction critical current than an in-plane field, by almost two orders of magnitude.

As an example, consider an AJTJ with circumference $C=0.5$ mm quenched at $\tau_Q=5$ s, for which dependence of the single fluxon trapping frequency $\bar{f}_1$ on an external field is shown in figure 3. Unsurprisingly, applying an external field in either direction makes the creation of a single fluxon more likely, leading to a double peak. If there is no stray field, then the central minimum occurs at $B=0$.

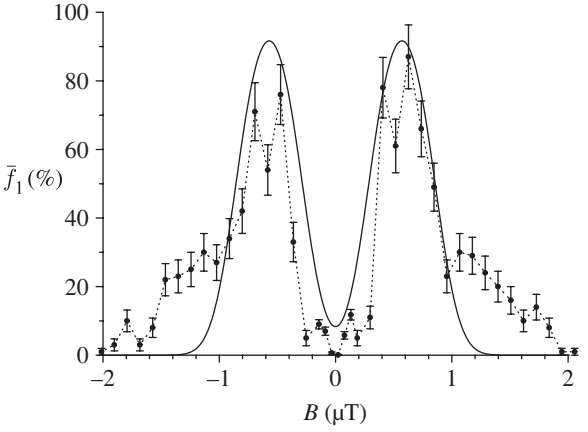

Figure 3. Dependence of the single fluxon trapping frequency $\bar{f}_1$ on quench time $\tau_Q = 5$ s for an AJTJ of circumference $C = 0.5$ mm in the presence of a magnetic field B perpendicular to the barrier plane. The error bars denote the statistical error from multiple thermal cycles (up to 300 per data point). The dotted line is a guide to the eye. The solid line does not correspond to a best fit near the minimum but follows from (3.4) for appropriate efficiency ϵ.

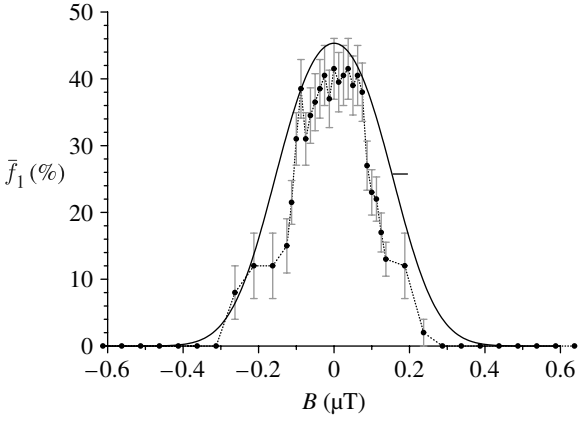

Figure 4. Dependence of $\bar{f}_1$ on quench time $\tau_Q = 5$ s for an AJTJ of circumference $C = 2.0$ mm in the presence of a magnetic field B perpendicular to the barrier plane. The error bars denote the statistical error from multiple thermal cycles (up to 300 per data point). The dotted line is a guide to the eye. The solid line follows from (3.4) for appropriate efficiency ϵ.

On other occasions (different τ_Q) it is displaced, showing the presence of a stray field. We generate a dataset of the form of figure 3 to create each data point in figure 2, whose values of $\bar{f}_1$ correspond to the values at the central minima.

However, the situation is much less clear when we look at the likelihood of finding a single (anti)fluxon in larger AJTJs in the presence of an external field. Figure 4 shows the results for a 2.0 mm long sample with the same J_c at the same quench time ($\tau_Q = 5$ s) as that of figure 3. Rather than the double peak of figure 3, we have only a central peak that looks counter-intuitive in that it does not permit scaling behaviour for $\bar{f}_1$.

In the remainder of this paper, we shall show how the results of figures 3 and 4 can be understood, and qualitatively predicted, in a framework that implies the scaling behaviour of figure 1. What follows is based on the results presented in our most recent paper (Monaco *et al.* 2008).

3. Gaussian probabilities and Gaussian correlations

There is another approach to the same scaling behaviour of (1.2) which is less obvious, but still commensurate with the notion of maximal rate of change. This is that the scaling behaviour is at least as much a reflection of the order parameter field being a predominantly Gaussian random variable as it is a simple consequence of causality. It has been realized for many years that assuming Gaussian *correlations* will lead to the KZ scaling laws of (1.2), without having to cite causality directly (Karra & Rivers 1997, 1998; Lythe & Moro 1999).

The reason is that second-order transitions are, in general, implemented through the exponential growth of the amplitudes of the unstable long-wavelength modes that control the field ordering. If this growth is fast enough, then the most important physics takes place before nonlinearities become important. For these untramelled Gaussian modes, this growth is controlled by the relevant causal speed and reflects the bounds of causality which its equations satisfy. Nonlinearities serve only to put a rapid brake on the system's evolution, leaving the Gaussian imprint intact.

However, it has to be said that, whereas the role of instabilities is well understood for single superconductors (Calcetta & Ibaceta 1999), we do not have a comparable understanding for JTJs. Nonetheless, however instabilities induce Gaussian correlations, we shall see that to assume such correlations provides a good characterization of the data of figures 3 and 4.

To understand how this happens, we first need to extend the prediction for $\bar{f}_1$ of (1.4), valid only for $C<\bar{\xi}$, across the whole range of $C/\bar{\xi}$. Initially, suppose that there is no external symmetry-breaking field. The Kibble mechanism suggests that a first guess as to how $\bar{f}_1$ behaves for $C\gg\bar{\xi}$ is to divide the annulus into $N\sim C/\bar{\xi}\geq 2$ domains of size comparable to $\bar{\xi}$, in each of which the Josephson phase ϕ is a constant. We assume that there is no correlation between the values of ϕ in adjacent domains but, in calculating the total phase change $\Delta\phi$ around the annulus, the shortest path in the phase (geodesic rule) will be taken when jumping from one domain to the next.

Let $G_N(\Delta\phi)$ be the probability that the change in phase ϕ is $\Delta\phi$ after N domain boundaries, with $G_1(\Delta\phi)=1/2\pi$ for $|\Delta\phi|<\pi$, zero otherwise. On increasing N, $G_N(\Delta\phi)$, which is determined by $N-1$ self-convolutions of G_1, shows rapid convergence to the Gaussian distribution that arises from the central limit theorem, already good at $N=2$.

For N not too small, the obvious way to proceed is to adopt this Gaussian distribution. That is, we assume that the total phase change $\Delta\phi$ around the annulus can be expressed as the sum of a random term ϕ and a geodesic-rule correction $\delta\phi$. If ϕ has a normal distribution with average $\bar{\phi}=0$ and variance $\sigma^2(N)$, i.e.

$$G_N(\phi)=\frac{1}{\sqrt{2\pi\sigma^2(N)}}\exp-\left(\frac{\phi^2}{2\sigma^2(N)}\right), \tag{3.1}$$

then a simple calculation enables us to identify (3.1) with the central limit distribution of the self-convolutions of G_1, as described above, provided $\sigma^2(N) = N\pi^2/3$. The probability to trap a net number m of defects will now be

$$f_m(N) = \int_{-\pi+2m\pi}^{\pi+2m\pi} \mathrm{d}\Phi\ G_N(\phi). \tag{3.2}$$

However, equation (3.2) does not give the required linear behaviour in $C/\bar{\xi}$ for $\bar{f}_1$ of (1.4) when continued to small N, when the approximation breaks down.

To recover this linear behaviour, we recall our earlier comments and assume, instead, that the winding number (fluxon) density $n(x) = \partial_x\phi(x)/2\pi$ is a *Gaussian random variable*. We now find that, instead of (3.2),

$$f_1(N) = f_{-1}(N) \approx \frac{1}{2\pi}\int_{-\pi}^{\pi} \mathrm{d}z\, \exp(-z^2\sigma(N)^2/8\pi^2)\cos z. \tag{3.3}$$

For *large* N, $\bar{f}_1$ from (3.3) is *identical* to that obtained from (3.2), while giving the required linear behaviour for small N.

In fact, although Gaussian probabilities follow from the Kibble mechanism and Gaussian correlations from the growth of linear instabilities, the two methods match remarkably well across the whole N range, apart from very small N, as do the expressions for f_0, the probability of seeing no fluxons. (Unfortunately, the periodicity of the ring makes it difficult to find an analytic approximation for f_m with Gaussian correlations when $m>1$.)

Let us now apply a perpendicular uniform magnetic field B to the ring. Once superconducting, the AJTJ expels most of the magnetic field, but a small fraction $\epsilon(B)$ of the applied field 'leaks' in the radial direction through the barrier. The effect of this field is to produce a non-zero average winding number $\langle n\rangle = \bar{n}(B)$. For an AJTJ, the field that penetrates the barrier will be given by the difference of the magnetic fluxes through the upper and lower rings $\bar{\phi}(B) = 2\pi\bar{n}(B) \propto \epsilon(B)C^2B$.

In the presence of external fields, we are not primarily interested in the small N linear regime and it is sufficient to work with Gaussian probabilities, rather than the almost identical Gaussian correlations. The natural extension of $G(\phi)$ of (3.1) for an AJTJ in a perpendicular magnetic field B is that the phase distribution will still be normal with variance $\sigma^2(N, \bar{n}(B))$, where we retain the definition of $N \sim C/\bar{\xi}$ given earlier, but with non-zero average $\bar{\phi}(B) = 2\pi\bar{n}(B)$. Using a mixed notation,

$$G_{N,\bar{n}}(\phi) = \frac{1}{\sqrt{2\pi\sigma^2(N)}}\exp -\frac{(\phi-\bar{\phi}(B))^2}{2\sigma^2(N)}. \tag{3.4}$$

As before, we are primarily interested in the probability of seeing a single fluxon or antifluxon, but now for fixed τ_{Q} (or N), as a function of B (or $\bar{n}$). With $f_{\bar{n}-m}(\bar{n}) = f_{\bar{n}+m}(\bar{n}) = f_{\pm m}(0)$, we repeat the identification $\sigma^2(N)/4\pi^2 = N/12$. Now $f_{+1}(\bar{n}) \neq f_{-1}(\bar{n})$. More precisely, in figure 5 we show $\bar{f}_1(N, \bar{n})$ as a function of $\bar{n}$ for fixed N for several N, as derived from Gaussian distribution equation (3.4).

The main characteristics of figure 5 are the following.

— For $N < N_{\mathrm{c}} \approx 10$ there is a double peak. This is understood as follows: essentially, when, for a given field B we have $\bar{n} = 1$, the zero-field no-trapping frequency $f_0(0)$ becomes the single fluxon trapping $f_{+1}(1) = f_0(0)$, giving the right-hand peak for positive $\bar{n} \approx 1$; reversing the field, $f_{-1}(-1) = f_0(0)$ and we

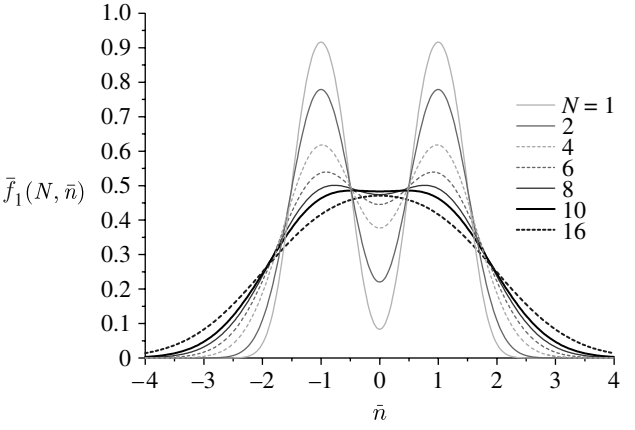

Figure 5. The values of $\bar{f}_1(N, \bar{n})$ as a function of $\bar{n}$ for fixed N for several values of N, N=1, 2, 4, 6, 8, 10 and 16, according to equation (3.4).

get the peak for negative $\bar{n} \approx -1$. The minimum value of $\bar{f}_1$ between the peaks is $\bar{f}_1(N)$, as given by (1.2).

— As N increases to N_c the height drops, the variance increases and the two peaks in $\bar{n}$ of $\bar{f}_1(N, \bar{n})$ merge at $N = N_c$ at the value $\bar{f}_c \approx 0.5$. This same N_c is the value of N for which $\bar{f}_1(N)$, the probability of seeing a fluxon or antifluxon with *no* external field, is maximized. The reason why the probability of seeing a *single* fluxon *decreases* for large N as N increases is a consequence of an increased ability to create more than one fluxon, making (1.4) inappropriate, with $C/\bar{\xi} > 1$.

— As N increases beyond N_c, there is only a single peak centred on $\bar{n} = 0$. Similarly, the reason why the probability of seeing a single fluxon decreases for large N as $|B|$ increases is also the consequence of it being easier to create more than one fluxon.

For appropriate ϵ, the curves in figure 5 for N=1 and 20 bear strong resemblance to the experimental data shown in figures 3 and 4, respectively. They comply with the most simple quantitative test of our analysis that the double peaks in figure 3 occur at a higher frequency than $\bar{f}_c \approx 50\%$, and the single peak in figure 4 at a lower frequency than 50%. More specifically, we note that the 2.0 mm long sample should be 16 times more sensitive to the externally applied magnetic field B if $\epsilon(B)$ is independent of B and identical for both samples. There is, indeed, a strong difference in sensitivity, but only by a factor of 7–8, showing that these assumptions are approximate. Further, the efficiency factor relating N to C has to vary by a factor of 5 between the samples. To fit the data profiles better we need specific properties of JTJs, beyond the generics of Gaussianity. This can be done (Martucciello & Monaco 1996), but it only adds unnecessary complexity at the level of discussion here.

4. Conclusions

We have argued that, in trying to understand the role of causality in transitions, the scaling behaviour of (1.2) is not the whole picture. Rather, we suggest that causal bounds arise through the order parameter (winding number density) being

a Gaussian random variable, which can be thought of as a consequence of instabilities growing as fast as possible.

In doing so, we have distinguished Gaussian *probabilities* that follow from the Kibble mechanism from the Gaussian correlations that follow from the Gaussian nature of the order parameter. The two are effectively identical where both are applicable, but only the latter leads to the scaling behaviour (1.4).

However, when describing defect formation in the presence of an external field, we can use either. The Gaussian approximation provides a better than qualitative explanation for fluxon production in an external field, as we pass from the regime of figure 3 with $C/\bar{\xi} < 1$, in which applying an external field leads to a greater likelihood of seeing an individual fluxon, to that of figure 4, in which the scaling law (1.4) is invalid because $C/\bar{\xi} > 1$.

We thank Arttu Rajantie of Imperial College for his helpful discussions.

References

Barone, A. & Paterno, G. 1982 *Physics and applications of the Josephson effect*. New York, NY: Wiley.

Calcetta, E. & Ibaceta, D. 1999 Counting defects in an instantaneous quench. *Phys. Rev. E* **60**, 2999–3008. (doi:10.1103/PhysRevE.60.2999)

Golubov, A. A., Houwman, E. P., Gijsbertsen, J. G., Krasnov, V. M., Flokstra, J., Rogalla, H. & Kupriyanov, M. Y. 1995 Proximity effect in superconductor–insulator–superconductor Josephson tunnel junctions: theory and experiment. *Phys. Rev. B* **51**, 1073–1089. (doi:10.1103/PhysRevB.51.1073)

Hindmarsh, M. & Rajantie, A. 2000 Defect formation and local gauge invariance. *Phys. Rev. Lett.* **85**, 4660–4663. (doi:10.1103/PhysRevLett.85.4660)

Karra, G. & Rivers, R. J. 1997 Initial vortex densities after a temperature quench. *Phys. Lett. B* **414**, 28–33. (doi:10.1016/S0370-2693(97)01155-6)

Karra, G. & Rivers, R. J. 1998 Reexamination of quenches in He-4 (and He-3). *Phys. Rev. Lett.* **81**, 3707–3710. (doi:10.1103/PhysRevLett.81.3707)

Kavoussanaki, E., Monaco, R. & Rivers, R. J. 2000 Testing the Kibble–Zurek scenario with annular Josephson tunnel junctions. *Phys. Rev. Lett.* **81**, 3452–3455. (doi:10.1103/PhysRevLett.85.3452)

Kibble, T. W. B. 1976 Topology of cosmic domains and strings. *J. Phys. A* **9**, 1387–1398. (doi:10.1088/0305-4470/9/8/029)

Kibble, T. W. B. 1980 Some implications of a cosmological phase transition. *Phys. Rep.* **67**, 183–199. (doi:10.1016/0370-1573(80)90091-5)

Lythe, G. & Moro, E. 1999 Dynamics of defect formation. *Phys. Rev. E* **59**, R1303. (doi:10.1103/PhysRevE.59.R1303)

Martucciello, N. & Monaco, R. 1996 Annular Josephson tunnel junctions in an external magnetic field: the statics. *Phys. Rev. B* **53**, 3471–3481. (doi:10.1103/PhysRevB.53.3471)

Monaco, R., Mygind, J. & Rivers, R. J. 2002 Zurek–Kibble domain structures: the dynamics of spontaneous vortex formation in annular Josephson tunnel junctions. *Phys. Rev. Lett.* **89**, 080 603. (doi:10.1103/PhysRevLett.89.080603)

Monaco, R., Mygind, J. & Rivers, R. J. 2003 Spontaneous fluxon formation in annular Josephson tunnel junctions. *Phys. Rev. B* **67**, 104 506. (doi:10.1103/PhysRevB.67.104506)

Monaco, R., Mygind, J., Aaroe, M., Rivers, R. J. & Koshelets, V. P. 2006*a* Zurek–Kibble mechanism for the spontaneous vortex formation in Nb–Al/Al-ox/Nb Josephson tunnel junctions: new theory and experiment. *Phys. Rev. Lett.* **96**, 180 604. (doi:10.1103/PhysRevLett.96.180604)

Monaco, R., Mygind, J., Aaroe, M., Rivers, R. J. & Koshelets, V. P. 2006*b* Experiments on spontaneous vortex formation in Josephson tunnel junctions. *Phys. Rev. B* **74**, 144 513. (doi:10.1103/PhysRevB.74.144513)

Monaco, R., Mygind, J., Aaroe, M., Rivers, R. J. & Koshelets, V. P. 2008 Spontaneous fluxon production in annular Josephson tunnel junctions in the presence of a magnetic field. *Phys. Rev. B* **77**, 054 509. (doi:10.1103/PhysRevB.77.054509)

Zurek, W. H. 1985 Cosmological experiments in superfluid helium. *Nature* **317**, 505. (doi:10.1038/317505a0)

Zurek, W. H. 1996 Cosmological experiments in condensed matter systems. *Phys. Rep.* **276**, 177–221. (doi:10.1016/S0370-1573(96)00009-9)